KIF3A Is a New Microtubule-based Anterograde Motor in the Nerve Axon

Satoru Kondo, Reiko Sato-Yoshitake, Yasuko Noda, Hiroyuki Aizawa, Takao Nakata, Yoshiharu Matsuura,* and Nobutaka Hirokawa

Department of Anatomy and Cell Biology, School of Medicine, University of Tokyo, Hongo, Tokyo 113, Japan; and *Laboratory of Hepatitis Viruses, Department of Virology II, National Institute of Health, Shinjuku-ku, Tokyo 162, Japan

Abstract. Neurons are highly polarized cells composed of dendrites, cell bodies, and long axons. Because of the lack of protein synthesis machinery in axons, materials required in axons and synapses have to be transported down the axons after synthesis in the cell body. Fast anterograde transport conveys different kinds of membranous organelles such as mitochondria and precursors of synaptic vesicles and axonal membranes, while organelles such as endosomes and autophagic prelysosomal organelles are conveyed retrogradely. Although kinesin and dynein have been identified as good candidates for microtubule-based anterograde and retrograde transporters, respectively, the existence of other motors for performing these complex axonal transports seems quite likely. Here we characterized a new member of the kinesin superfamily, KIF3A (50-nm rod with globular head and tail), and found that it is localized in neurons, associated with membrane organelle fractions, and accumulates with anterogradely moving membrane organelles after ligation of peripheral nerves. Furthermore, native KIF3A (a complex of 80/85 KIF3A heavy chain and a 95-kD polypeptide) revealed microtubule gliding activity and baculovirus-expressed KIF3A heavy chain demonstrated microtubule plus end–directed (anterograde) motility in vitro. These findings strongly suggest that KIF3A is a new motor protein for the anterograde fast axonal transport.

NEURONS are highly polarized cells composed of cell bodies and long cytoplasmic processes (i.e., an axon and dendrites). Because of the lack of protein synthesis machinery in the axon and because many materials are synthesized in the cell body, highly developed intracellular transport mechanisms are required for the maintenance of the axon. Axonal transports are divided into two flows, fast and slow, with the fast flow possessing both anterograde and retrograde directions. Fast anterogradely transported materials are tubulovesicular structures, membrane-associated proteins, neuropeptides, neurotransmitters, and associated enzymes, whereas prelysosomal vesicles, multivesicular bodies, multilamelar bodies, growth factors, and recycled proteins are transported retrogradely. Mitochondria are transported bidirectionally at a different fast velocity (Grafstein and Forman, 1980; Brady, 1991; Hirokawa, 1991; Hollenbeck, 1993). These functions must be carried out by motor proteins.

Kinesin is a motor enzyme first identified in the squid axoplasm and now isolated from a variety of cell types (Scholey et al., 1985; Vale et al., 1985; Neighbors et al., 1988; Saxton et al., 1988). Kinesin could move microtubules along a glass surface or translocate Latex beads on microtubules in vitro; the movement of microtubule segments and Latex beads showed that kinesin is a plus end–directed motor protein (Vale et al., 1985; Saxton et al., 1988). Vesicle transport was affected by the introduction of antibodies against kinesin into the axoplasm (Brady et al., 1990). Immunofluorescence microscopy studies of cultured cells (Hollenbeck, 1989; Pfister et al., 1989) showed the colocalization with vesicle-like structures, and further study using ligated peripheral nerves showed that kinesin was abundantly associated with anterogradely transported membrane-bound organelles (Hirokawa et al., 1991). Genetic and in vivo analyses of the kinesin heavy chain have been performed in *Drosophila.* The mutants defective in the kinesin heavy chain of *Drosophila* caused behavioral abnormality and, although there was no reduction in neurite length, this suggested the requirement of kinesin for normal neuromuscular function (Saxton et al., 1991). Furthermore, the same kinesin mutation in *Drosophila* affected the action potential propagation in axons and neurotransmitter release at nerve terminals (Gho et al., 1992). In the axon various different kinds of membranous organelles are conveyed bidirectionally at different rates. In addition, there is also a variety of structures of crossbridges between membranous organelles and microtubules in vivo that are candidates for motor molecules (see Hirokawa, 1982; Hirokawa et al., 1985; Hirokawa and Yorifuji, 1986). These

Address all correspondence to N. Hirokawa, Department of Anatomy and Cell Biology, School of Medicine, University of Tokyo, Hongo, Tokyo, 113 Japan.

data indicated that kinesin is a good candidate for a fast axonal transporter, but also suggested the existence of other motors mediating the fast axonal transport.

Recently, several genes were discovered whose predicted products were related to kinesin (for reviews see Endow, 1991; Goldstein, 1991; Bloom, 1992; Hirokawa, 1993). The region of their similarity corresponds to the kinesin motor domain which includes a putative ATP-binding site and a region that can bind to microtubules (Yang et al., 1989; Enos and Morris, 1990; Hagan and Yamigada, 1990; Kosik et al., 1990; McDonald and Goldstein, 1990; Meluh and Rose, 1990; Zhang et al., 1990; Endow and Hatsumi, 1991; Otsuka et al., 1991). This superfamily of kinesin-like, microtubule-based motor proteins appears to have diverse motility functions such as mitosis (Scholey et al., 1985; Leslie et al., 1987; Enos and Morris, 1990; Hagan and Yanagida, 1990; Hoyt et al., 1992; Roof et al., 1992) and meiosis (Endow et al., 1990; McDonald and Goldstein, 1990; Zhang et al., 1990). From these findings of the diversity of kinesin, the possibility exists that there are some unknown axonal transporters that are kinesin-like. Indeed, the UNC-104 from nematode *Caenorhabditis elegans*, a novel member of the kinesin superfamily with a kinesin-like motor domain, has been demonstrated to be a putative neuron-specific motor used for the anterograde axonal transport of synaptic vesicles (Hall and Hedgecock, 1991).

Therefore, we speculated about the existence of several other new members of kinesin-like proteins in mammalian neuronal cells. We have previously cloned five different members from their homology to the kinesin motor domain by PCR method (Aizawa et al., 1992). KIF3A (formerly designated as KIF3) (701 amino acids) is a member of this kinesin superfamily and is an as yet unidentified new species. Northern blot analysis showed that KIF3A is predominantly expressed in brain, although trace amounts of KIF3A transcript were detected in various tissues. The motor-like domain of KIF3A is located at the NH_2 terminus, the alpha-helical domain at the middle, and the proline-rich globular domain at the COOH terminus.

To better understand the role of the KIF3A protein in neurons and to determine whether it is really a microtubule-based motor, we characterized KIF3A by immunological, immunocytochemical, biochemical, and molecular biological approaches. Further, to investigate the differences between kinesin and KIF3A, the molecular structure and pharmacological characteristics of KIF3A were examined. Microtubule gliding activity was measured using baculovirus-expressed KIF3A and native KIF3A 80/85 kD and a 95-kD polypeptide complex. In addition, we determined its immunolocalization in the brain and in cultured neurons and investigated its accumulation by ligating peripheral nerves at the light microscopic level. The results strongly suggest that KIF3A is really a microtubule-dependent motor protein mediating the anterograde fast axonal transport in neurons, and that this is the first finding of the existence of a new anterograde motor other than kinesin that works in mammalian axons.

Materials and Methods

Construction of Transfer Vector

Complete KIF3A cDNA, which was originally cloned into pUC19 (Aizawa et al., 1992), was reintroduced into pBluescript SK(+) at the EcoRI site (pBS/KIF3A). A transfer vector was constructed using the pAcYM1 transfer vector (Matsuura et al., 1987) which contains the viral polyhedrin promoter for the expression of the cloned cDNA insert. To generate pAcYM1/KIF3A, the EcoRV site was introduced just upstream of the initial ATG start codon of the KIF3A cDNA in the pBS/KIF3A by PCR method. The KIF3A cDNA was excised by digestion with EcoRV and EcoRI and repaired with the Klenow fragment of DNA polymerase I. This EcoRV–EcoRI fragment encodes the entire coding region of KIF3A including the termination codon. The blunt-ended EcoRV–EcoRI fragment was ligated into the dephosphorylated SmaI site of the pAcYM1 transfer vector. The junction sites were sequenced and determined to contain the ATG codon and termination codon of KIF3A.

Transfection and Selection of Recombinant Virus

The insect cell line Spodopetra frugiperda (Sf9)[1] was propagated in TC100 medium (GIBCO BRL, Gaithersburg, MD) supplemented with bactotryptose broth and 10% fetal bovine serum (Summers and Smith, 1987). AcRP23.lacZ virus DNA (Kitts et al., 1990) was used because the replacement of the β-galactosidase gene by cDNA in the pAcYM1 vector can be detected in the presence of X-gal. Sf9 cells were transfected with mixtures of linearized AcRP23.lacZ DNA and pACYM1/KIF3A by lipofection (GIBCO BRL) to generate recombinant baculovirus AcKIF3A containing KIF3A cDNA resulting from homologous recombination. After 4 d of incubation at 27°C, supernatant fluids were harvested and assayed for recombinant virus by infecting Sf9 monolayers and overlaying them with agarose. A few days later, recombinant plaques were selected in the presence of the substrate X-gal. The plaques were picked out and the recombinant virus was purified by two rounds of screening in the presence of X-gal and grown to high titer stocks by serial amplification. The purified recombinant virus stock of high titration (10^7 plaque-forming U/ml) was used to infect monolayers of Sf9 cells for the subsequent recombinant KIF3A expression.

Expression and Purification of KIF3A Protein

For expression of the KIF3A protein, Sf9 cells were infected with AcKIF3A at a multiplicity of 1–10 PFU/cell and incubated at 27°C for 72 h. Cells were harvested by centrifugation and washed once with PBS. Each 10 ml of cell culture was resuspended in 1 ml of PEM buffer (0.1 M Pipes, pH 6.8, 1 mM EGTA, and 1 mM $MgCl_2$) supplemented with 1 mM DTT, 1 mM PMSF, and 10 μg/ml leupeptin. The cells were then lysed with a glass-teflon homogenizer and clarified with a Beckman TL100 ultracentrifuge at 100,000 *g* for 30 min (Beckman Instrs. Inc., Fullerton, CA). The resulting supernatant was referred to as the cell extract.

The KIF3A protein was purified by microtubule affinity and sucrose gradient centrifugation as follows. The cell extract was mixed with microtubules (0.5 mg/ml), 20 μM taxol, and 2 mM AMP-PNP, incubated at room temperature for 30 min, and centrifuged in a microfuge at top speed for 10 min. The KIF3A protein was released from microtubules by resuspending the pellet in 1/10 volume of PEM buffer (containing 10 mM ATP, 0.5 M KCl, or both 10 mM ATP and 0.5 M KCl), and then incubating at room temperature for 30 min, followed by centrifugation at 100,000 *g* for 15 min at 20°C. The supernatant containing the enriched KIF3A protein eluted by ATP was further purified by sucrose gradient centrifugation. The concentrated protein was loaded on 5–20% linear sucrose gradients of 13 ml. The gradients were centrifuged at 31,000 rpm for 16 h at 2°C. 5-ml fractions were collected and analyzed by SDS-PAGE (Laemmli, 1970). The peak fraction was used for further analysis. As controls, Sf9 cells infected with parent virus not expressing KIF3A were used.

Motility Assay

Translocation of microtubules was observed as described by Vale et al. (1985). For the baculovirus-expressed KIF3A, 1 μl of tenfold diluted KIF3A peak fraction, consisting of ~10 ng of KIF3A protein in the case of peak fraction (concentration was diluted to 100-fold), 1 μl of 0.3% casein and 5 μl of PEM buffer were mixed and adsorbed onto a glass cover slip. For the native KIF3A, 6 μl of each fraction of superose S6 column chromatography and 1 μl of 0.3% casein were used instead. In the case of native KIF3A fractions the motility was assayed in the presence or absence of SUK4 monoclonal antibody (kind gift from Dr. Scholey, University of California, Davis, CA) (Ingold et al., 1988), an antibody against sea urchin egg kinesin.

1. *Abbreviations used in this paper*: MT, microtubule; PVDF, polyvinylidene difluoride; Sf9, Spodopetra frugiperda.

After 10-min incubation, 1 μl of Mg^{2+}-ATP (at an appropriate concentration), 1 μl of taxol (final 20 μM), and 1 μl of phosphocellulose-purified porcine brain microtubules (final 10 μg/ml) were added. The cover slip was inverted on the glass slide and sealed with nail lacquer. Motility was monitored by video-enhanced DIC microscopy with a ZEISS axiophot microscope (Carl Zeiss, Inc., Thornwood, NY), Hamamatsu ARGUS-10 image processor (Hamamatsu Corp., Bridgewater, NJ), and SONY EVO 9650 8-mm video tape recorder. A video recording of a 20 × 20-μm field of microtubules (MTs) was made over 2 min, and the velocities of MTs were determined over distances of 5 μm. The polarity of movement was judged from the direction of the movements of Chlamydomonas axonemes, which were prepared as described by Witman (1986). For estimating the motility activity of the KIF3A expressed and the control fractions, the numbers of attached, slightly attached, and gliding MTs were counted from the video recording of a 20 × 20-μm field of 2 min, and then the ratio of gliding MTs to total MTs was calculated.

Low Angle, Rotary Shadowing EM

The purified KIF3A protein solutions were mixed with ammonium acetate and glycerol at concentrations of 0.5 M and 50%, respectively. They were then sprayed onto freshly cleaved mica flakes, followed by vacuum drying as described previously (Tyler and Banton, 1980; Hirokawa, 1986). Rotary shadowing with platinum was performed at an angle of 6° using a Balzers (Hudson, NH) model 301 freeze fracture apparatus, and the replicas were processed further as described previously (Hirokawa et al., 1988). All specimens were observed and photographed with a JEOL 2000 EX electron microscope at 100 kV (JEOL U.S.A. Inc., Peabody, MA).

The dimensions of various domains of KIF3A molecules were determined by quantitative morphometric methods as described previously (Hirokawa et al., 1989). Micrographs were printed at a magnification of 140,000×.

Polyclonal Antibody Production

For the antigen, recombinant KIF3A protein was expressed in *Escherichia coli* using a PET3d vector with the full-length KIF3A cDNA. Overexpressed KIF3A protein was loaded onto SDS-PAGE and the band corresponding to KIF3A protein was cut out of the preparative gel. 500 μg of excised KIF3A protein was mixed with complete Freund's adjuvant and injected into the axial lymph nodes of two rabbits. The rabbits received three booster shots with 250 μg of excised KIF3A mixed with incomplete Freund's adjuvant at 14-d intervals. On the third day after the third booster, the rabbits were bled from the ear vein and tested by immunoblotting analysis. Subsequently, this serum was affinity purified using a KIF3A-bound triopropyl-Sepharose 6B affinity column.

Monoclonal Antibody Production

Crude extract of Sf9 cells overexpressing KIF3A protein was incubated with taxol-polymerized MTs and centrifuged at 100,000 *g* for 30 min. Tubulin pellet including 100 μg of KIF3A was emulsified with Freund's adjuvant and injected into mice intraperitoneally every two weeks. After three or four injections, mouse spleen cells were fused with P3-653 myeloma cells using 50% polyethylene glycol 4000 (Kohler and Milstein, 1976). Wells grown in HAT (hypoxanthine-aminopterin-thymidine) medium were screened by ELISA and immunoblotting. After limiting dilutions and screenings, hybridoma cultures that secreted antibodies against KIF3A were cloned.

Western Blot Analysis

Equal amounts of crude homogenates from various mouse tissues were fractionated on 7.5% SDS-PAGE and transferred to polyvinylidene difluoride (PVDF) membranes in a Tris–glycine buffer, 20% methanol (Towbin et al., 1979). The filters were dried, washed several times with TBS (10 mM Tris, pH 7.5, 150 mM NaCl), and blocked for 1 h in TBS containing 5% BSA. The filters were incubated for 1 h at 37°C with the primary antibodies (at 1:1000 dilution) in TBS containing 5% BSA. The filters were then washed five times (10 min each) in TBS containing 0.05% Tween 20, and incubated with the secondary alkaline phosphatase-conjugated antibodies (goat anti-rabbit IgG, at 1:1000 dilution) for 1 h at 37°C. Following five washes with TBS and 0.05% Tween 20, the blots were developed with bromochloro-iodolylphosphate (15 μl of a 50 mg/ml stock) and nitroblue tetrazolium (2.5 μl of a 75 mg/ml stock) in 10 ml of alkaline phosphatase-detection buffer (100 mM Tris, 100 mM NaCl, 5 mM $MgCl_2$, pH 9.5).

Total homogenates of P7 mouse brain were loaded on 7.5% SDS-PAGE and transferred to PVDF membranes. The sheets were blocked with 5% BSA and stained with culture supernatant of anti-KIF3A monoclonal antibody and 1:100 anti KIF3A polyclonal antibody and detected with 1:100 peroxidase-conjugated anti-mouse and anti-rabbit antibody, respectively, in 50 mM Tris-HCl buffer (pH 7.6) containing 0.5 mg/ml 4-chloronaphthol and 0.03% H_2O_2.

Immunofluorescence Microscopy of Mouse Cerebellum, Cerebrum, Spinal Cord, and Cultured Spinal Cord Neurons

Female albino mice (7 d postnatal) were anesthetized and transcardially perfused with 2% paraformaldehyde and 0.1% glutaraldehyde in 0.1 M cacodylate buffer, pH 7.2. Cerebella, hippocampus, and spinal cord were dissected out, further fixed in the same fixative for 2 h, and cryoprotected with a graded series of sucrose PBS. 10-μm cryosections were processed for immunofluorescence microscopy by using affinity-purified anti-KIF3A polyclonal IgG (10–20 μg/ml) or anti-KIF3A monoclonal antibody. Preimmune rabbit serum containing equivalent amounts of IgG or normal mouse IgG were used as the first antibody for controls.

Spinal cord neurons were cultured from 12-d-old mouse embryos as described previously (Ransom et al., 1977; Okabe and Hirokawa, 1989). Cells were fixed with cold methanol for 5 min at −20°C, washed with PBS, and double stained with affinity-purified anti-KIF3A antibody and anti-MAP 2 monoclonal antibody (Sato-Yoshitake et al., 1989) as the first antibodies, and with rhodamine-labeled anti-rabbit IgG goat IgG and fluorescein-labeled anti-mouse IgG goat IgG as the second antibodies. Preimmune rabbit serum and normal mouse IgG were used as the first antibodies for controls.

Ligation of Mouse Peripheral Nerves

Sciatic nerves of anesthetized 3-wk-old female albino mice were ligated tightly with surgical threads, and the animals were kept in small cardboard boxes to severely restrict their movement. After 6 h, the mice were transcardially perfused with 2% paraformaldehyde and 0.1% glutaraldehyde in 0.1 M cacodylate buffer, pH 7.2, as described previously (Hirokawa et al., 1990). Small pieces of nerves both proximal and distal to the ligated portions were frozen by liquid freon after cryoprotection with graded series of sucrose PBS and were sectioned on a cryostat (4–5 μm). The sections were stained with affinity-purified anti-KIF3A antibodies (~20 μg/ml). Normal rabbit IgG, preimmune serum containing equivalent amounts of IgG, and anti-KIF3A IgG after absorption with KIF3A peptides expressed in *E. coli* (precipitated) were used as first antibodies for control. Recombinant KIF3A protein was expressed in *E. coli* using a PET3d vector with the full-length KIF3A cDNA. KIF3A protein expressed in the *E. coli* system was mainly condensed in precipitation.

Sections were preincubated for 1 h with 5% skim milk PBS and stained using rhodamine-labeled anti-rabbit IgG as the second antibodies as described previously (Hirokawa et al., 1990). Sections from proximal and distal regions were treated similarly and photographed with a Zeiss Axiophoto fluorescence microscope and printed at the same condition. These experiments were carried out seven times using a total of 21 mice.

Subcellular Localization of KIF3A

Rat brain was homogenized by a teflon homogenizer with 10 × vol of ice-cold 0.32 M sucrose, 10 mM Hepes (pH 7.4). The homogenate was centrifuged at low speed (3,000 *g*) for 10 min at 4°C. The supernatant was centrifuged at medium speed (9,200 *g*) for 15 min. The medium speed supernatant was again centrifuged at high speed (100,000 *g*) for 60 min. The supernatant was collected as cytosolic fraction (S3). The low (P1), medium (P2), and high (P3) speed pellets were homogenized again with the sucrose buffer and centrifuged at the same speeds. The protein concentration of each fraction was analyzed by BCA method (PIERCE, Rockford, IL). These P1, P2, P3, and S3 fractions were subjected to electrophoresis and transferred to PVDF membrane. The effect of salt extraction was examined by incubating the P2 and P3 fractions with 0.5 M NaCl or KI in 0.32 M sucrose buffer for 30 min at 4°C. These salt-extracted homogenates were centrifuged at 100,000 *g* for 60 min, and pellets were analyzed by immunoblotting. The 0.5 M salt-washed P3 fraction was further applied to a 0.6–1.2 M sucrose density gradient at 38,000 rpm for 2 h in a Beckman SW40Ti rotor. 1-ml fractions were collected from 13-ml tubes. The same volume from each fraction was applied to SDS-PAGE and transferred to PVDF membrane. Fractions were analyzed by immunoblotting with affinity-purified anti-KIF3A polyclonal antibody and anti-kinesin monoclonal antibody (H2; a

kind gift from Dr. George S. Bloom, University of Texas Southwestern Medical Center, Dallas, TX).

PC12 cells were grown in DME supplemented with 5% horse serum and 5% FBS. The cells were grown to half-confluence and then dibutyryl cAMP and NGF at concentrations of 1 mM and 10 ng/ml, respectively, were added. Three days later, the cells were harvested in the above buffer and homogenized by glass-teflon homogenizer for 20 strokes. The homogenates were centrifuged at 3,600 *g* for 10 min and the supernatant was ultracentrifuged at 100,000 *g* for 1 h to collect the membrane vesicles. The pellet was resuspended and loaded onto a sucrose gradient (0.35–2 M) and centrifuged at 25,000 rpm, (Beckman, type SW40Ti rotor) at 4°C for 22 h. 1-ml fractions were collected from 13-ml tubes. The same volume from each fraction was applied to SDS-PAGE and transferred to PVDF membrane. Fractions were analyzed by immunoblotting with affinity-purified anti-KIF3A polyclonal antibody, anti-kinesin monoclonal antibody (H2), and anti-P38 (synaptophysin) (Boehringer Mannheim Corp., Indianapolis, IN).

Measurement of the Amounts of KIF3A, Kinesin, and Tubulin in Mouse Brain

Brains were dissected from adult mice and homogenized in 2 vol of buffer (100 mM Pipes, pH 6.6, 1 mM $MgCl_2$, 1 mM EGTA, 5% 2-mercaptoethanol, 10% glycerol, and 4% SDS). The sample was boiled for 5 min, centrifuged for 10 min at 10,000 *g* at 2°C, separated by SDS-PAGE on 7.5% gels, and then transferred onto nitrocellulose sheets. Purified baculovirus-expressed KIF3A, kinesin from rat brain, and tubulin from porcine brain were loaded onto the same sheets as the concentration standards. The concentrations of standard KIF3A and kinesin were determined by SDS–gel densitometry using bovine serum albumin as a control, as described before (Sato-Yoshitake et al., 1992). The concentration of tubulin was estimated by the assay of Bradford (1976). The sheets were immunoblotted using affinity-purified polyclonal anti-KIF3A antibody, anti-kinesin monoclonal antibody (H2), or anti-tubulin monoclonal antibody (DM1A; Sigma Chem. Co., St. Louis, MO), followed by incubation with ^{125}I-protein A for KIF3A or ^{125}I-anti-mouse IgG for kinesin and tubulin (ICN Biomedicals, Costa Mesa, CA). The quantitation of protein concentration was performed with a BAS 2000 Image Analyzer (Fuji Photo Film Co. Ltd., Tokyo, Japan).

Purification of Native KIF3A from Porcine Brain

7-d-old porcine brains were used. The total brain was homogenized with a Waring blender in an equal volume of PEM buffer solution supplemented with 1 mM PMSF, 10 μg/ml leupeptin, 1 mM DTT, and 0.5 mM GTP. The homogenate was centrifuged at 15,000 *g* for 30 min, 1/4 vol of glycerol was added and the solution was incubated for 40 min at 37°C. This solution was then centrifuged at 35,000 *g* for 40 min at 30°C, and the supernatant was dialyzed against 20 PE (20 mM PIPES, pH 6.8, and 2 mM EGTA) overnight at 4°C and then centrifuged at 15,000 *g* (600 ml). The supernatant was then loaded on a DEAE-cellulose column equilibrated with 20 PE. After unabsorbed materials were washed out with the same buffer solution, a linear gradient of NaCl (from 0 to 0.3 M, total 4,800 ml) in 20 PE was applied, collecting 30-ml fractions. The content of KIF3A in each fraction was checked by Western blot. DEAE-cellulose column fractions containing KIF3A were mixed and solid ammonium sulfate was added (final saturation 70%). Precipitates formed were collected by centrifugation and dissolved in ~60 ml of PEM buffer. After dialysis against PEM buffer, the fraction was centrifuged at 15,000 *g* for 15 min. The supernatant was supplemented with 0.1 mM GTP, 17 μM taxol, and 0.5 mg/ml tubulin, and incubated at 37°C for 5 min to allow the tubulin to polymerize. After the addition of 1 mM AMP-PNP, the solution was further incubated at 37°C for 10 min to allow KIF3A to bind to microtubules. The microtubule suspension was layered onto PEM buffer containing 10% (wt/vol) sucrose and 17 μM taxol. Microtubules containing KIF3A were collected by centrifugation at 20,000 *g* for 20 min, and the pellet was washed with PEM buffer containing 20 μM taxol. KIF3A was eluted by suspending and homogenizing the microtubules in 7 ml of PEM buffer containing 15 mM Mg^{2+}–ATP, 0.2 M NaCl, 20 μM taxol, and 0.5 mM GTP, and incubating the suspension at 37°C for 15 min. After removing the microtubules by centrifugation at 100,000 *g* for 20 min, the supernatant was dialyzed against 20 PE and supplemented with 0.1 mM GTP, 33 μM taxol, 1 mg/ml tubulin, and 1 mM AMP-PNP, and incubated at 37°C for 15 min. The microtubule suspension was layered onto PEM buffer containing 10% (wt/vol) sucrose, and 33 μM taxol and centrifuged at 20,000 *g* for 20 min. The pellet was washed with PEM buffer containing 20 μM taxol and KIF3A was eluted by suspending microtubules in 1 ml of PEM buffer containing 15 mM Mg^{2+}–ATP, 0.1 M NaCl, 33 μM taxol, and 0.5 mM GTP. After incubating at 37°C for 10 min, the suspension was centrifuged at 100,000 *g* for 15 min. The supernatant was applied to superose S6 column chromatography (Pharmacia LKB, Uppsala, Sweden) pre-equilibrated with PEM buffer and eluted with the same buffer solution, collecting fractions of 0.5 ml. The fractions that contained significant amounts of KIF3A were applied to a DEAE-cellulose column again. A linear gradient of NaCl (from 0 to 0.3 M, total 24 ml) in PEM was applied, collecting 0.5-ml fractions. The content of KIF3A in each fraction was checked by SDS-PAGE. DEAE-cellulose column fractions containing KIF3A were mixed and dialyzed against PEM, followed by centrifugation at 100,000 *g* for 30 min to remove insoluble materials. The ratio of the 95-, 85-, and 80-kD polypeptide was estimated by densitometric analysis using Shimadzu CS-9000 dual wavelength flying-spot scanner (Shimadzu, Tokyo, Japan).

Results

Expression and Purification of Recombinant KIF3A Protein

To investigate whether KIF3A protein is indeed a microtubule motor, a baculovirus expression system was used because KIF3A protein expressed in an *E. coli* system was mainly condensed in the precipitation and had no activity. The full-length of KIF3A cDNA was introduced into the transfer vector pAcYM1, and then recombinant baculoviruses were generated by cotransfection followed by homologous recombination. KIF3A protein was expressed under the polyhedrin promoter with the level of expression being highest at day 3 after infection and reaching about 30% of the total insect cell proteins (10 mg of recombinant KIF3A protein was obtained from 1×10^9 Sf9 cells) (Fig. 1 *A*). Approximately half of the KIF3A protein was soluble following cell homogenization and clarification (Fig. 1 *A*). To investigate the activity, a MTs-sedimentation assay was used for these soluble proteins. Recombinant KIF3A protein cosedimented with MTs in the presence of AMP-PNP and was released from MTs in the presence of Mg^{2+}–ATP (Fig. 1 *A*). We used this assay for the first purification step. This fraction was contaminated with kinesin, dynein, and perhaps other motor proteins originally expressed in the Sf9 cells. By sucrose gradient purification, high molecular weight motor proteins were eliminated and the peak fraction of KIF3A (Fig. 1 *B*, lane *5*) was distinct from the peak fraction of Sf9 kinesin (Fig. 1 *B*, lane *7*). The band of Sf9 kinesin was invisible by Coomassie Brilliant Blue staining but was barely detectable by silver staining (data not shown).

Most of the KIF3A protein was released from the MTs pelleted with ATP, but some remained on the MTs. We therefore tried to determine whether the remaining KIF3A would be released by the addition of KCl. Almost no KIF3A was eluted by buffer alone (Fig. 1 *A*, lanes *6* and *10*) or by 0.5 M KCl buffer (Fig. 1 *A*, lanes *8* and *12*). Further, the eluted portion of the ATP buffer supplemented with 0.5 M KCl (Fig. 1 *A*, lanes *9* and *13*) was fairly similar to that of the ATP buffer (Fig. 1 *A*, lanes *7* and *11*). This result suggests that most of the solubilized KIF3A is active and that KIF3A–MTs binding is nucleotide dependent. The KIF3A protein remaining on MTs may be inactivated during the procedures.

Motility of KIF3A Protein

The baculovirus-expressed KIF3A fraction (Fig. 1 *B*) could translocate MTs reconstituted from taxol polymerized tubulin on a glass surface. As indicated in Fig. 1 *B*, this activity correlated well with the protein concentration of KIF3A but

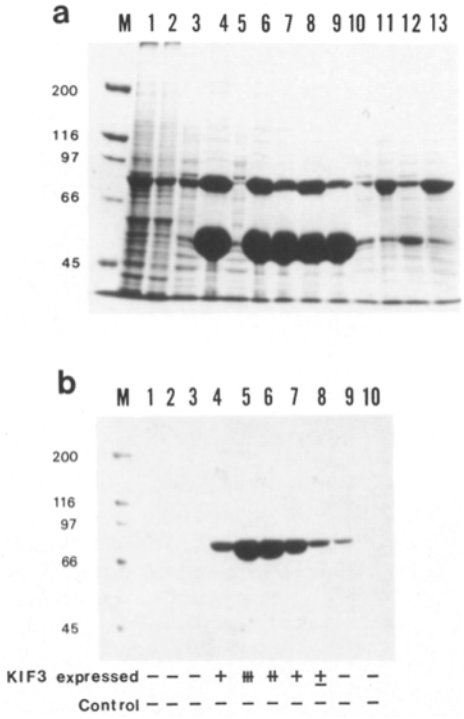

Figure 1. SDS-polyacrylamide gel electrophoresis demonstrating expression, microtubule sedimentation assay, and sucrose gradient purified fractions of KIF3A produced by recombinant baculovirus. (*a*) Sf9 cells were harvested 3 d after infection with recombinant virus AcKIF3A. Lane *M*, molecular size markers; lane *1*, total crude extract; lanes *2* and *3*, first pellet and clarified supernatant; lanes *4* and *5*, the pellet and supernatant of the clarified cell extract mixed with MTs in the presence of AMP-PNP; lanes *6* and *10*, the pellet and supernatant of buffer extraction; lanes *7* and *11*, the pellet and supernatant of Mg^{2+}-ATP extraction; lanes *8* and *12*, the pellet and supernatant of KCl extraction; lanes *9* and *13*, the pellet and supernatant of Mg^{2+}-ATP and KCl extraction. The arrowhead indicates the KIF3A protein. (*b*) Sucrose gradient fraction. 13 ml of 5 to 20% sucrose in PEM buffer was overlaid with ATP-released concentrated sample, and centrifuged at 31,000 rpm for 16 h in a Beckman SW 40 Ti swinging bucket rotor at 4°C. Fractions 1–10 correspond to 5 to 11.5% sucrose fractions. The arrowhead indicates KIF3A protein, and the arrow indicates tubulin. The motility activity of KIF3A expressed and control fractions were indicated by plus and minus signs. +++, ≥90%, ++, ≥70%, +, ≥50%, ±, ≥30%, −, ≈0%. The determination of this activity was described in Materials and Methods.

not that of kinesin in the sucrose gradient fractions. The similarly prepared fraction obtained from Sf9 cells infected with parent virus not expressing KIF3A had no activity to translocate MTs when assayed by the same method. The percentage of moving MTs using the peak fraction (Fig. 1 *B*, lane *5*) of KIF3A was 100%. At 1 mM Mg^{2+}-ATP, the rate of movement was 0.6 ± 0.1 μm/s (n = 43) at room temperature. To determine the direction of the movement of the MTs, axonemes were isolated from *Chlamydomonas*. *Chlamydomonas* axonemes moved only to the compact end (minus end) at a velocity of about 0.6 μm/s (n = 3) (Fig. 2), indicating that KIF3A is a plus end-directed motor and corresponds to the direction of transport toward the nerve terminal in axons. MTs motility mediated by KIF3A was shown to require Mg^{2+} as a cofactor for the nucleotide substrate. Mg^{2+}-ATP-dependent MTs motility was inhibited by EDTA, and MTs motility was absent in Mg^{2+}-free buffer containing Mg^{2+}-free ATP. An increase in the rate of MTs gliding was observed with ATP concentrations between 50 and 20 mM. Other nucleotide triphosphates were tested for MTs gliding induced by KIF3A. Among them, only GTP was substitutable, with the gliding activity of MTs being indistinguishable from the movement in the presence of ATP. CTP, ITP, and UTP were poor substrates for KIF3A activity, and the rate of MTs gliding was only about one third of the ATP-activated motility. KIF3A-driven MTs motility was inhibited by the addition of the nonhydrolyzable nucleotide analogue AMP-PNP in a dose-dependent manner in a range of 20 to 100 μM with half of the movement being abolished at a concentration of 70 μM AMP-PNP in the presence of 1 mM Mg^{2+}-ATP. We also examined the nonhydrolyzable nucleotide analogue ATPγS. In the presence of equimolar concentrations of ATP, MTs gliding was completely inhibited. With the addition of this analogue, MTs were firmly attached to the glass surface and did not move at all.

Other ATPase inhibitors were also tested. As for sodium vanadate, a phosphate analogue, the MTs motility was inhibited in a concentration-dependent manner. 10 μM vanadate did not show any obvious effect, but the MTs motility completely stopped at 70 μM, and half of the gliding was interrupted at 30 μM. Nonionic detergent Triton X-100 did not affect the KIF3A activity to translocate MTs at 0.1%. KIF3A was insensitive to NEM, although up to relatively high concentrations (1–50 mM) were investigated. DTT (2 mM) also did not affect the activity of KIF3A. These pharmacological data are summarized in Table I.

Molecular Structure of KIF3A

We analyzed the submolecular structure of KIF3A by low angle rotary shadowing and electron microscopy. Rotary-shadowed KIF3A exhibited a number of consistent morphological features. Most of the molecules were generally rod shaped and ~50 nm in length (mean 50.3 ± 4.8 nm, n = 116). One end of each molecule typically displayed one or two globular structures, referred to as head (long diameter of head, mean 10.3 ± 0.6 nm, n = 116) (Fig. 3). On the other hand, unlike kinesin, the opposite end, or tail, of the molecule had no characteristic structures. The head and tail regions were connected by a long shaft. In the majority of replicas, the shaft appeared relatively straight.

Western Blot Analysis for the Expression Pattern of KIF3A

To investigate the tissue-specific and developmental expression level of the KIF3A protein, we performed Western blot analysis of various mouse organs from 5-d-old (data not shown) and 3-wk-old mice (Fig. 4). We used affinity-purified polyclonal antibody and monoclonal antibody against KIF3A; these antibodies specifically reacted with KIF3A protein, and no cross-reaction among other KIFs was detected under the conditions used (Fig. 4 *b*). KIF3A was observed at a very high level in the extract of brain, and at a high level in the extract of testis. However, it was detected at a low level in kidney, lung, and pancreas, and faintly in heart, intestine, and liver (Fig. 4 *a*). The expression patterns were similar and the level of expression was equal in both 5-d-old and 3-wk-

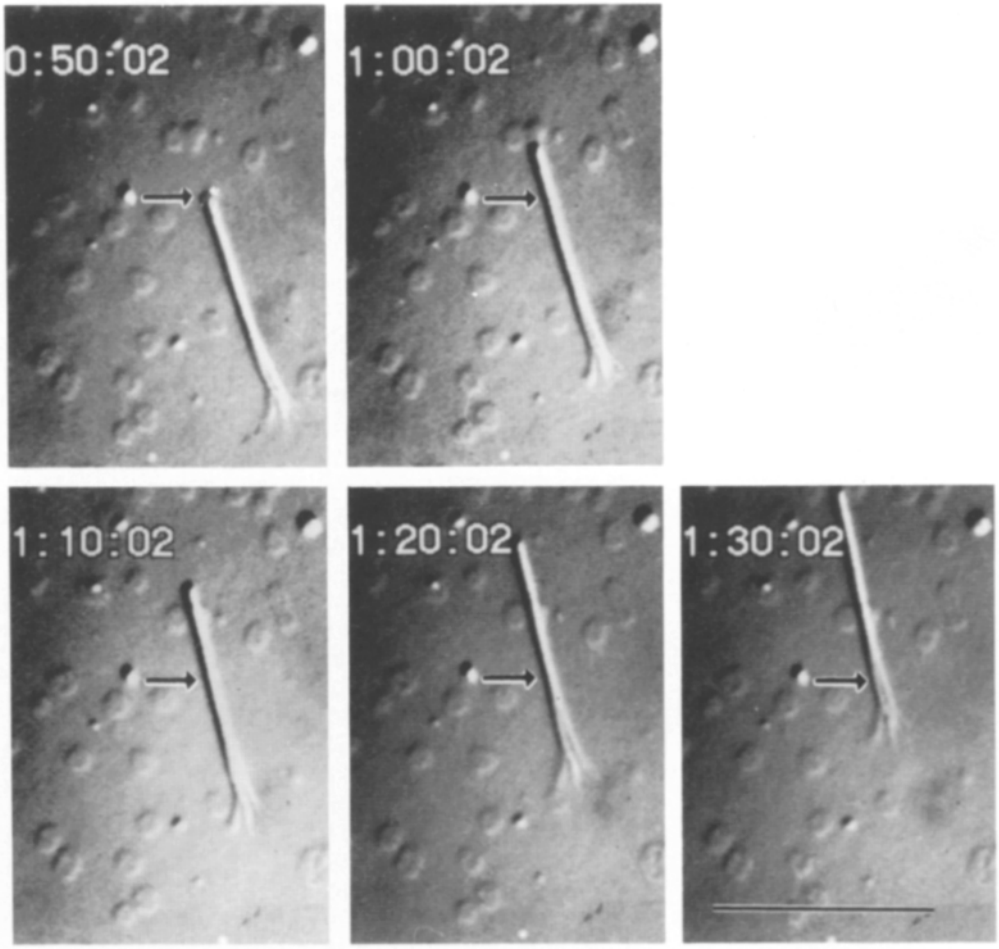

Figure 2. The direction of the movement produced by recombinant baculovirus-expressed KIF3A protein. Axonemes purified from *Chlamydomonas* were assayed for gliding activity on the surface of KIF3A coated cover slips. The axonemes glided toward their compact end, indicating plus end-directed motility activity of the KIF3A protein. The arrow in the subsequent panels was placed in the same position of the compact end. Bar, 10 μm.

old mice. The immunoreactive band of KIF3A from nervous tissues appeared as a doublet. The lower band corresponded to the band of KIF3A protein expressed by baculovirus, and we supposed that the upper band of KIF3A in the brain extract may be a posttranslational modified form of KIF3A or some other related protein of KIF3A.

Table I. Pharmacological Data

Substrate	Concentration/condition	Motility
ATP	50 μM–20 mM	+
CTP	1 mM	+
GTP	1 mM	+
ITP	1 mM	+
UTP	1 mM	+
ADP	1 mM	−
ATP γS	1 mM	−
AMP-PNP	0.02 mM	+
	0.07 mM	±
	0.1 mM	−
Vanadate	10 μM	+
	30 μM	±
	70 μM	−
NEB	1 mM–50 mM	+
DTT	2 mM	+
EDTA	2 mM	+
	5 mM	−
Triton X-100	0.1%	+
Azide	5 mM	+

Immunofluorescence Microscopic Localization of KIF3A in Nerve Tissues and Cultured Spinal Cord Cells

In the 7-d-old mouse cerebellum anti-KIF3A antibodies stained molecular layers mainly composed of abundant parallel fiber axons of inner granular cells. They also stained cell bodies and dendrites of Purkinje cells and neurons in the molecular layers as well as the cerebellar medulla mainly consisting of axons (Fig. 5). In addition, monoclonal antibody against KIF3A stained cell bodies of large neurons in the deep cerebellar nuclei. In the hippocampus and spinal cord large neurons such as pyramidal cells and motor neurons were also stained in a dot-like manner. They also stained other neurons in the cerebral cortex, hippocampus, cerebellar nuclei, and brain stem to a lesser degree (Fig. 5). Neurons in gray matter and axons in white matter of spinal cords were stained as well (Fig. 5). In spinal cord neurons in culture, polyclonal anti-KIF3A antibodies stained axons and cell bodies brightly and dendrites to a somewhat lesser degree (Fig. 5). Other cells such as glia cells and fibroblasts were not stained significantly. Collectively it was shown that KIF3A is localized in neurons, prominently in axons and cell bodies and also to a lesser degree in dendrites.

Localization of KIF3A in Ligated Peripheral Nerves

In previous studies it was demonstrated that anterogradely and retrogradely moving membranous organelles conveyed

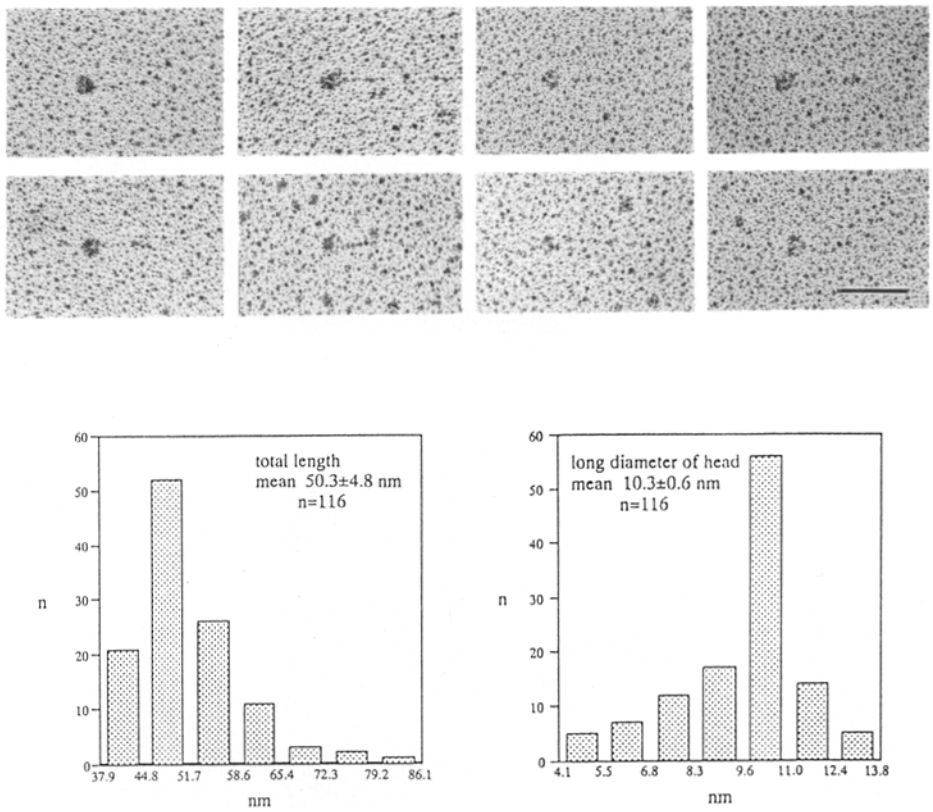

Figure 3. (*a*) KIF3A molecules observed by low angle, rotary shadowing EM. Several representative molecules are shown here. (*b*) Morphometric analysis of KIF3A. The total length and long diameter of the heads were measured for KIF3A molecules. Bar, 50 nm.

by fast axonal flow accumulate at the proximal and distal portions of axons, respectively, ~6 h after ligation of mouse peripheral nerves (Hirokawa et al., 1990, 1991). In the present study, proximal and distal portions of ligated sciatic nerves were stained with affinity-purified polyclonal antibodies against KIF3A. Immunofluorescence microscopy revealed that KIF3A antibody strongly and reproducibly stained regions of the nerves proximal to the ligation. In contrast, staining in regions distal to the ligated parts was significantly weaker than that seen on the proximal side (Fig. 6). A gradational pattern of staining on the proximal side was observed, becoming brighter as the regions were closer to the ligated portions. Furthermore, the diameter of the nerves tended to be somewhat greater near the ligated parts. In control, preimmune rabbit serum, normal rabbit IgG or affinity-purified KIF3A antibodies after absorption with KIF3A proteins expressed in *E. coli* were used as the primary antibodies, and only faint background staining was observed. These results indicate that peripheral nerve axons contain a certain amount of KIF3A and that KIF3A accumulates anterogradely

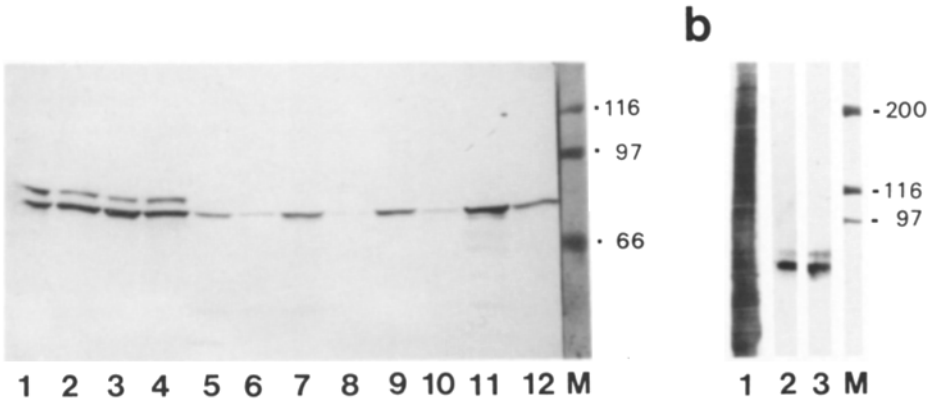

Figure 4. Expression pattern of KIF3A in various tissues from 3-wk-old mice. (*A*) Western blotting using anti-KIF3A affinity-purified IgG. Lane *1*, cerebrum; lane *2*, hippocampus; lane *3*, cerebellum; lane *4*, spinal cord; lane *5*, spleen; lane *6*, liver; lane *7*, kidney; lane *8*, heart; lane *9*, lung; lane *10*, small intestine; lane *11*, testis; lane *12*, pancreas; lane *M*, molecular mass marker. Molecular masses are indicated on the right side (kD). (*b*) Western blotting of mouse brain crude homogenates using anti-KIF3A affinity-purified rabbit IgG or an anti-KIF3A monoclonal mouse IgG. Lane *1*, CBB staining of mouse brain crude homogenate; lane *2*, anti-KIF3A monoclonal antibodies; lane *3*, anti-KIF3A rabbit IgG; lane *M*, molecular mass marker.

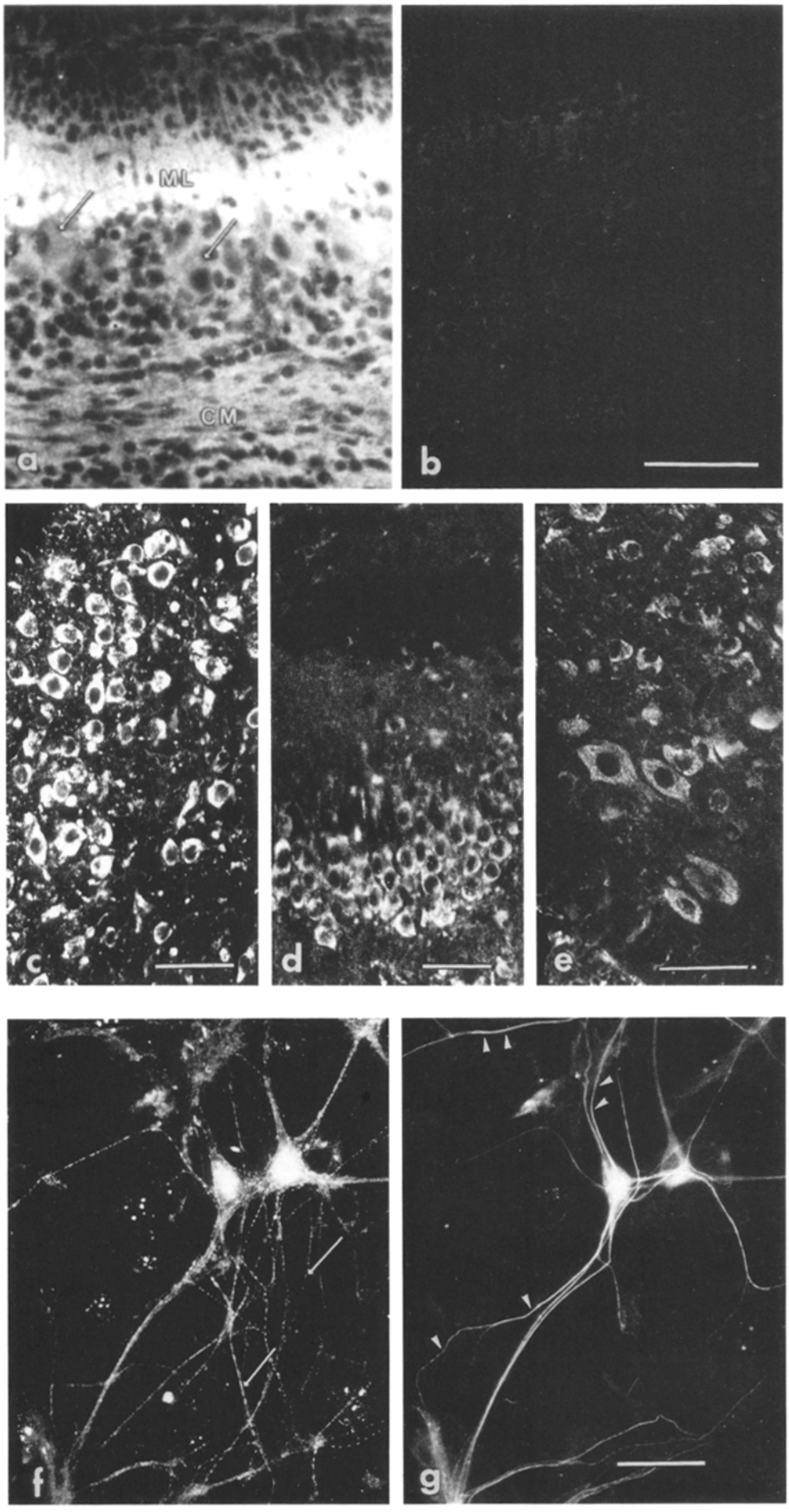

Figure 5. Immunofluorescence microscopy of 7-d-old mouse cerebellum (*a–c*), hippocampus (*d*), spinal cord (*e*), and cultured spinal cord neurons (*f* and *g*). *a* and *f* are stained with anti-KIF3A rabbit antibodies; *b* is stained with preimmune rabbit IgG; *c*, *d*, and *e* are stained with a mouse monoclonal anti-KIF3A antibody; *g* is stained with a monoclonal anti-MAP2 antibody. Anti-KIF3A antibodies stained the molecular layer composed of mainly parallel fiber axons (*ML*) predominantly, while they also stained the cerebellar medulla (*CM*), Purkinje cell bodies (*arrows*), and dendrites and other neurons (*a*). Anti-KIF3A antibodies also stained neurons in cerebellar nucleus (*c*), hippocampus (*d*), and spinal cords (*e*). Anti-KIF3A stained axons and cell bodies prominently (*f, arrow*), while staining of dendrites tended to be weak (see comparable dendrites with arrowheads in *g*). Dendrites and cell bodies were stained with anti-MAP2 monoclonal antibodies (*g*). Bars; (*a*, *b*, *f*, and *g*) 50 μm; (*c–e*) 20 μm.

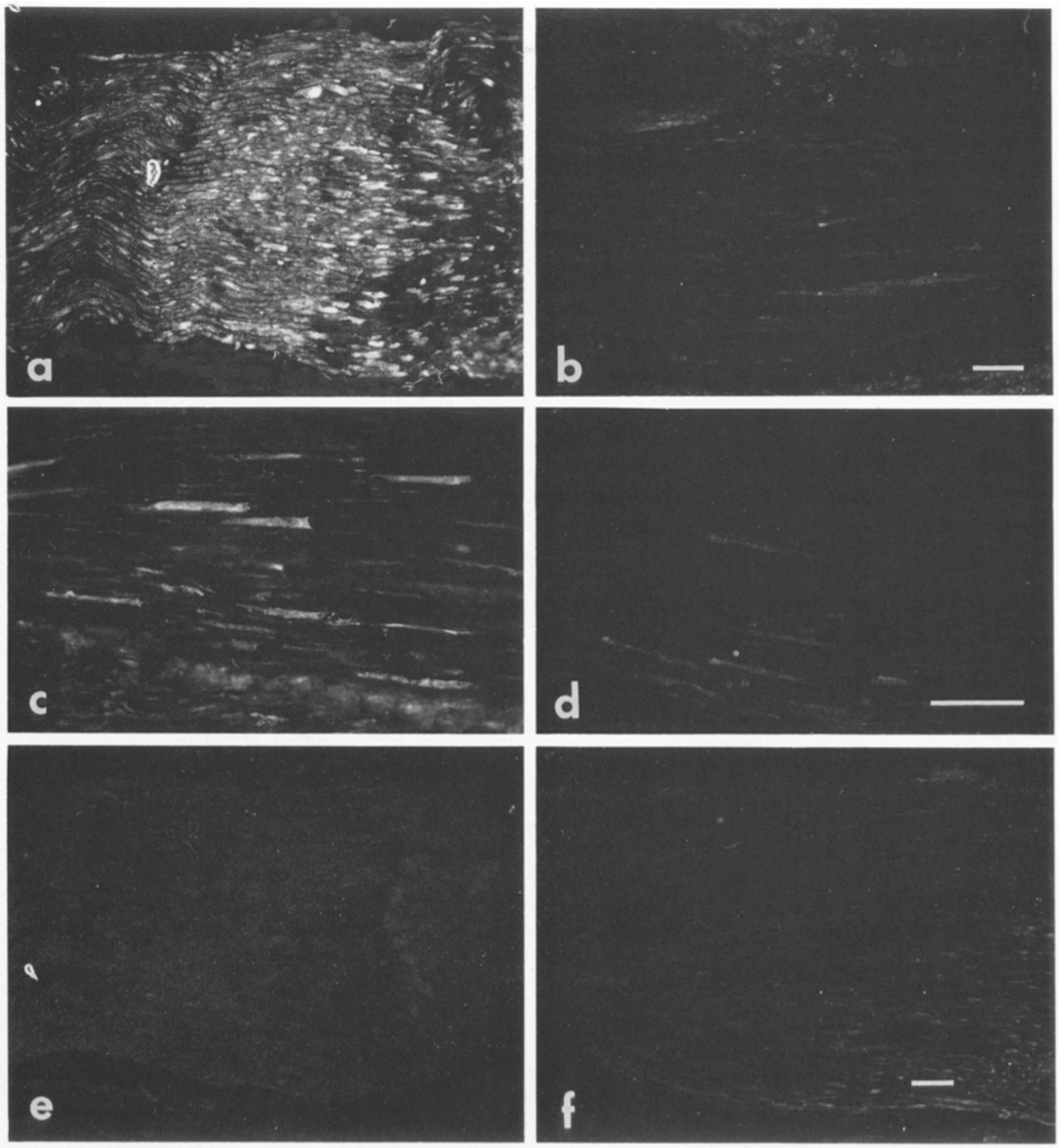

Figure 6. Immunofluorescence micrographs of mouse sciatic nerve sections stained with affinity-purified anti-KIF3A antibodies (*a–d*) or with preimmune IgG (*e* and *f*). *a*, *c*, and *e* are proximal, while *b*, *d*, and *f* are distal to the ligations. Anti-KIF3A antibodies stained proximal portions brightly whereas the staining at the distal portions was much less bright. Bars, 50 μm.

at the ligation, suggesting that this protein is associated to a considerable degree with anterogradely moving organelles in vivo.

Subcellular Localization of KIF3A

We have analyzed the subcellular localization of motor proteins by centrifuged sedimentation assay of rat brain homogenates. Immunoblotting demonstrated that there is no cross-reaction between KIF3A and kinesin or other KIFs. After low, medium, and high centrifugations, KIF3A and kinesin exist almost evenly in all the particulate fractions (data not shown). Previous studies showed that low speed pellets (P1) contain the nuclear fraction and mitochondria, medium speed pellets (P2) contain synaptosomes and lysosomes, and high speed pellets (P3) contain mostly microsomes (Ueda et al., 1979). We further defined whether KIF3A and kinesin bind tightly to the sedimented organelles. Medium and high speed pellets were extracted with 0.5 M

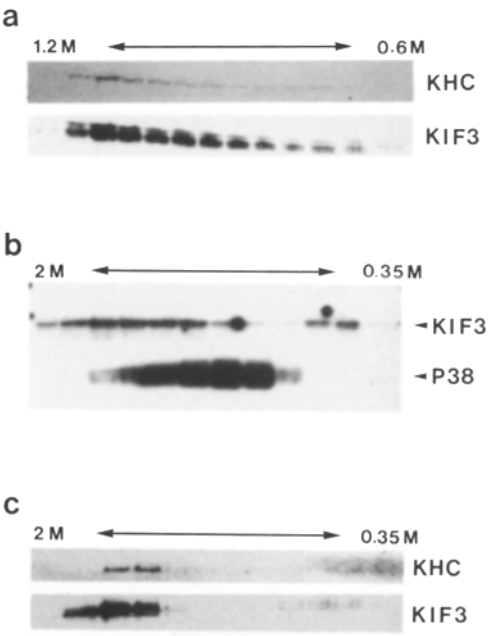

Figure 7. (*a*) The binding of KIF3A and kinesin to membrane vesicles. Microsome fraction from rat brain was fractionated by sucrose gradient centrifugation and analyzed by immunoblotting. Both KIF3A and kinesin were enriched in the heavy fractions and showed a similar pattern of distribution. Fractions from left to right ranged from 1.2 to 0.6 M sucrose. (*b* and *c*) The binding of KIF3A and kinesin to P38-containing vesicles. Particulate fraction from NGF-induced PC12 cells was fractionated by sucrose gradient centrifugation. The same volume from each fraction was applied to SDS-PAGE, transferred to PVDF membrane, and analyzed by immunoblotting. Anti-P38 (synaptophysin) antibody was used for the detection of the P38-containing vesicle fractions. The peak fraction of KIF3A was clearly distinct from that of synaptophysin, and also the peak fraction of kinesin was almost the same as that of KIF3A. Fractions from left to right ranged from 2 to 0.35 M sucrose.

NaCl or KI in 0.32 M sucrose buffer. Considerable amounts of KIF3A and kinesin remained in the particulate fraction even after salt extraction (data not shown), as previously described in squid kinesin (Schnapp et al., 1992). The subcellular localization of KIF3A was similar to that of kinesin, while the ratio of cytosolic KIF3A to the particulate fraction was somewhat higher than that of kinesin (data not shown).

The washed microsome fraction (P3) was further fractionated by sucrose gradient centrifugation and analyzed by Western blotting. In the microsome fractions, kinesin and KIF3A were both enriched in the heavy fractions and their distribution was similar (Fig. 7 *a*). To avoid the possibility that cell fractionation of a mixture of various types of cells may disturb the clear separation of membrane fractions, we used membrane fractions obtained from NGF-induced PC12 cells. PC12 cells were homogenized and then P2 and P3 fractions were mixed and applied to sucrose gradient centrifugation. The blot was stained with the antibody against small clear vesicle membrane protein P38 (synaptophysin). The staining overlapped somewhat, but the peak fraction of KIF3A was clearly distinct from the peak of P38 (Fig. 7 *b*). The second KIF3A peak at a lower sucrose gradient would represent free KIF3A segregated from the membrane fraction (Fig. 7 *b*), because this peak coincided with that of the purified protein (Fig. 1 *b*) and also because a similar peak was observed when nonwashed microsome fractions from brain were analyzed by sucrose density gradient.

Thus, KIF3A and kinesin were mainly associated with membrane organelles other than vesicles containing P38 (Fig. 7, *b* and *c*), although they did show similar fractionation patterns. It should be noted, however, that the fraction peak for P38-containing vesicles (P38 is associated with clear synaptic vesicles in brain synaptosomes, while it is associated with clear small vesicles in PC12 cells in which synaptic vesicles are cored vesicles and contain monoamine) (Navone et al., 1986) represents mainly the clear vesicles in the terminals (the final destination of the cargoes) of PC12 cells, and not the transported form of clear vesicle precursors (which may be small in population).

Quantitative Analysis of Kinesin and KIF3A in the Mouse Brain

To compare the concentrations of KIF3A and kinesin in the nerve tissues, we measured the amount of these proteins in mouse brain crude extracts. The concentration of KIF3A was 0.64 ± 0.11 μg/mg ($n = 3$) of total proteins, and that of kinesin was 4.43 ± 0.82 μg/mg ($n = 3$) of total proteins. The molar ratios of tubulin to KIF3A and to kinesin were 1351:1 and 198:1, respectively. Therefore the amount of KIF3A was about one seventh compared to that of kinesin.

Purification of Native KIF3A Protein

7-d-old porcine brains were used for the source of KIF3A. A DEAE-cellulose column was used for the first step of the purification. Electrophoresis of the fraction showed that KIF3A was a minor component and could not be identified by CBB staining (Fig. 8 *a*), and therefore the content of KIF3A in the fraction resulting from subsequent steps was monitored by Western blot using polyclonal anti-KIF3A antibody (Fig. 8 *b*). KIF3A was eluted with 0.15 mM NaCl and concentrated by ammonium sulfate precipitation. The concentrated fraction was cosedimented with MTs in the presence of AMP-PNP and eluted with ATP. More than 90% of the polypeptides with molecular weights of 80,000, 85,000, and 120,000 in the ammonium sulfate fraction cosedimented with MTs, and about 70% of the polypeptides were released from MTs by ATP (Fig. 8 *a*, lane *4*). The band at the molecular weight of 120,000 might be kinesin (Fig. 8 *a*). The ATP eluate fraction was cosedimented with MTs in the presence of AMP-PNP and released by ATP again. The final ATP-released fraction was applied to superose S6 column chromatography (Fig. 8 *c*). The final eluted fraction contained significant amounts of kinesin heavy chain, together with 95-, 85-, and 80-kD polypeptides (Fig. 8 *c*). Fractions that contained relatively high amounts of KIF3A were subjected to DEAE-cellulose column chromatography once more (Fig. 8 *a*, lanes *11* and *12*). We observed that the 80/85-kD polypeptides immunoreactive against anti KIF3A antibodies always copurified with a 95-kD polypeptide that does not react with KIF3A affinity-purified polyclonal antibody (Fig. 8 *a*, lanes *11* and *12* and *c*, lanes *20* and *21*). We also estimated the ratio of 95-, 85-, and 80-kD polypeptide by densitometric analysis. The resulting ratio was ~2:1:1 for each polypeptide. Because sea urchin KRP (85/95) resembling KIF3A forms a complex with a 115-kD nonimmunoreactive band which does not have ATPase activity (Cole et al., 1993) the

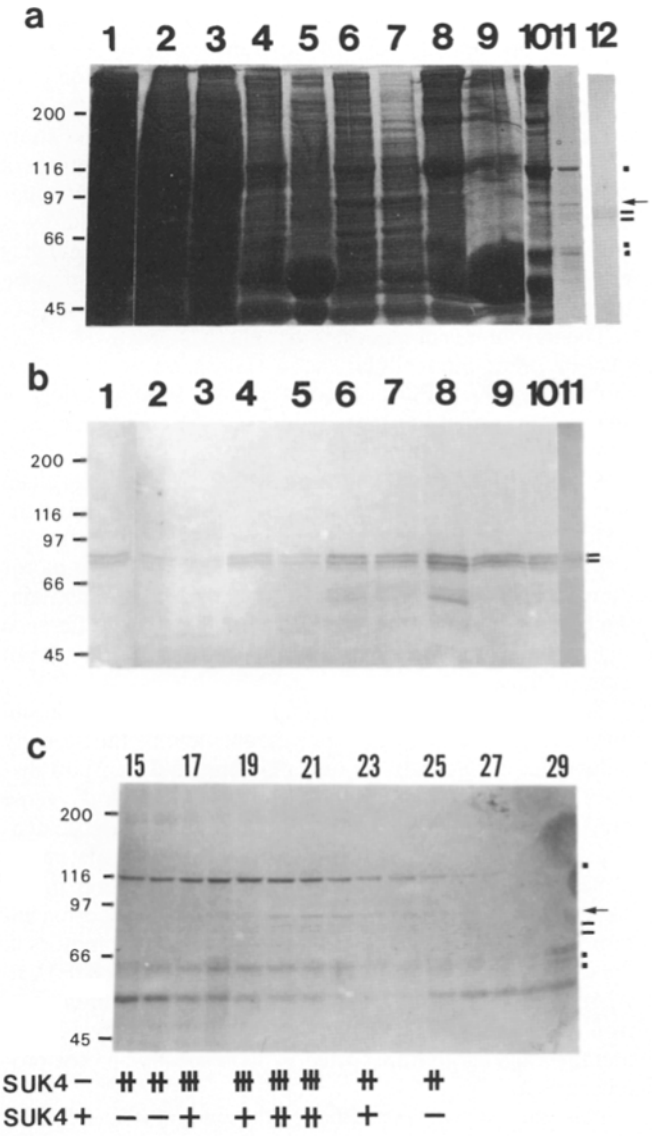

Figure 8. Semipurification steps of porcine KIF3A. (*a*) Gel electrophoresis of proteins in fractions obtained during the course of purification. Gels were stained with 0.1% CBB (lanes *1–11*) or immunoblotted with anti-KIF3A antibodies (lane *12*). (*b*) Immunoblotting of the fractions obtained during the course of purification of KIF3A with anti-KIF3A antibodies. Lane *1*, crude extract of porcine brain; lane *2*, first DEAE-cellulose column chromatography fraction enriched with KIF3A; lane *3*, first cycle supernatant not cosedimented with MTs in the presence of AMP-PNP; lane *4*, first cycle ATP-eluted supernatant; lane *5*, first cycle ATP noneluted MTs pellet; lane *6*, dialysate of first cycle ATP-eluted supernatant; lane *7*, second cycle supernatant not cosedimented with MTs in the presence of AMP-PNP; lane *8*, second cycle ATP-eluted supernatant; lane *9*, second cycle ATP noneluted MTs pellet; lane *10*, superose S6 gel filtration column chromatography fraction enriched with KIF3A; lanes *11* and *12*, second DEAE-cellulose column chromatography fractions enriched with KIF3A (80/85 kD). (*c*). Superose S6 gel filtration of semi-purified KIF3A (80/85 kD). 80/85 kD immunoreactive bands are always copurified in a single peak with a 95-kD polypeptide that does not react with anti-KIF3A antibodies. Motility assay was performed in the absence (*SUK 4−*) or presence (*SUK 4+*) of monoclonal antibody against KHC (SUK 4). Fraction numbers are on the top of each lane. In the presence of SUK 4 monoclonal antibody each the remaining activity coincided with the strength of the band of KIF3A and not of kinesin.

80/85-kD polypeptides may also form a complex with the 95-kD polypeptide.

Motility Assay of Native KIF3A Protein

To determine whether the 80/85-kD polypeptides stained with polyclonal anti-KIF3A antibody have indeed MTs translocational activity, motility assay was performed using gel filtration fractions (Fig. 8 *c*). Fractions after the final purification still contain a small amount of kinesin, but the application of SUK4 monoclonal antibody (kind gift from Dr. Scholey) (Ingold et al., 1988), an antibody against sea urchin egg kinesin, could block the motor activity of kinesin at least at the kinesin concentrations in lanes *15* and *16* of Fig. 8 *c*. In the presence of SUK4, the profile of microtubule gliding activity corresponded to the concentration of the 80/85-kD polypeptides and not to the 120-kD kinesin polypeptide. Furthermore, motility was observed in the presence of SUK4 antibody in fraction 23, where the kinesin concentration was below that found in fractions 15 and 16. These results suggest that the native 80/85/95 complex can produce motility. The velocity of movement was similar to that produced by KIF3A expressed in Sf9 cells.

Discussion

KIF3A Is a Microtubule Plus End-directed Motor Having Distinct Characteristics from Kinesin

We have previously cloned and sequenced the KIF3A gene from the murine nervous system whose predicted protein product at its amino terminus was homologous to the ATPase-containing and MTs-binding globular regions of the kinesin heavy chain but had little amino acid sequence similarity to the other parts of this molecule (Aizawa et al., 1992). Analysis of KIF3A by low angle, rotary shadowing showed that KIF3A is composed of a globular head domain (~10 nm in diameter) and a rod-like tail domain (~40 nm in length). This structural data coincided with the prediction based on the primary structure which suggests that KIF3A is mainly composed of the NH_2-terminal globular motor domain and alpha-helix-rich rod domain. Kinesin has a globular head at one end and a fan-like tail at the other (Hirokawa et al., 1989; Scholey et al., 1989; Yang et al., 1989). These ends are linked by an alpha-helical rod domain (Yang et al., 1989). Compared with kinesin (~80 nm long), KIF3A shows several distinct characteristics. KIF3A is much shorter (~50 nm) than kinesin. This could be mainly due to the shorter alpha-helical domain of KIF3A. Another difference is the end of the rod domain. Although kinesin has a fan-like tail, KIF3A does not show such a prominent structure. This could be partially based on the existence of light chains in the case of kinesin while KIF3A in this study consists of only heavy chains. KIF3A protein purified from porcine brain appeared as a 80/85-kD doublet and copurified

The motility activity of fractions were indicated by plus and minus signs. +++, ≥90%, ++, ≥70%, +, ≥50%, ±, ≥30%, −, ≈0%. The determination of this activity is described in Materials and Methods. (*a–c*) The left side numbers, molecular masses (kD). The right side: double lines, KIF3A (80/85 kD); arrows, 95-kD polypeptide; Single square, kinesin heavy chain; double square, kinesin light chains.

with a 95-kD polypeptide that did not react with anti-KIF3A antibodies. This suggests that the native KIF3A protein may have an associated protein as well, which may function in regulating the binding of KIF3A to membrane organelles.

Concerning the characteristics of KIF3A as a motor protein, the present study indicated that KIF3A could bind to MTs in the presence of AMP-PNP and be released in the presence of ATP. Further, from the in vitro motility assay, KIF3A promoted the translocation of MTs toward the minus end of MTs, indicating that KIF3A is an MT plus end-directed motor. Although the direction of MT motility, velocity (0.6 μm/sec), and some pharmacological characteristics were similar to those of kinesin (Vale et al., 1985), KIF3A was much more sensitive to AMP-PNP than kinesin in terms of blockage of the motility. These results in total suggest that KIF3A is an MT plus end-directed motor distinct from kinesin. Native KIF3A protein appeared as a 80/85-kD doublet, copurified with a 95-kD polypeptide and displayed motile activity along MTs. Our immunoprecipitation study using anti-KIF3A antibody indicated that KIF3A 80/85-kD polypeptides form a complex with 95-kD polypeptide (H. Yamazaki, Y. Okada, T. Nakata, Y. Noda, and N. Hirokawa, manuscript in preparation). Therefore in vivo KIF3A may reveal motile activity as a complex with a 95-kD polypeptide.

KIF3A Is a Putative Anterograde Motor for Fast Axonal Transports

Western blot analysis of various tissues showed that KIF3A is predominantly expressed in brain. Our immunofluorescence study indicated the localization of KIF3A in neurons, and predominantly in axons and cell bodies. Consequently it must be assumed that KIF3A has some function in neuronal activity.

Until now, three classes of mechanochemical ATPases have been identified in the nervous system: kinesin, cytoplasmic dynein and myosins (Espreafico et al., 1992). Kinesin moves objects toward the microtubule plus end (Vale et al., 1985) and dynein toward the minus end (Paschal et al., 1987). Because axonal microtubules are mainly oriented with plus ends away from the cell body, these results lead to the hypothesis that kinesin represents the anterograde motor and dynein the retrograde motor for fast organelle transport. Indeed, both are attached to the membrane surfaces of organelles in the axon, and the accumulation of kinesin is preferentially seen on the proximal side of a ligation, whereas cytoplasmic dynein accumulates both on the proximal and distal sides of the ligation (Hirokawa et al., 1990, 1991). Our present study demonstrated the preferential accumulation of KIF3A on the proximal side of ligated axons, where anterogradely moving membranous organelles accumulate. With regard to the total amount of KIF3A in brain, the molar ratio of KIF3A to kinesin was ~1:7, supporting the idea that KIF3A, as well as kinesin, may function as a motor for the fast anterograde axonal transport.

We further analyzed the subcellular localization of KIF3A and compared it with that of kinesin by centrifuged sedimentation assay of rat brain homogenates. Considerable amounts of KIF3A and kinesin remained in the particulate fraction even after salt extraction (0.5 M NaCl or KI in 0.32 M sucrose buffer) (Fig. 7), as previously described in squid kinesin (Schnapp et al., 1992). Because KIF3A is a plus end-directed motor, these results again strongly suggest that KIF3A also functions for the anterograde organelle transport systems. Among membranous organelles, synaptic vesicles or their precursors seem to be transported by a neuron specific motor (unc-104) for anterograde translocation in *C. elegans* as unc-104 null mutants showed a phenotype with axons having few synaptic vesicles. A recent antisense study demonstrated that kinesin may transport a certain group of membranous organelles (Navone et al., 1992). Whether each type of membranous organelles is conveyed by a specific type of motor or whether there is some redundancy among several distinct types of motors is still an open question.

The tail domain of kinesin is thought to interact with vesicular or other intracellular cargo (Hirokawa et al., 1989; Goldstein, 1991). Purification of kinesin from a variety of sources revealed it to generally be a tetramer containing two heavy chains and two light chains (Bloom et al., 1988). The EM study of kinesin demonstrated that kinesin light chain was located in the tail domain that probably contains the COOH terminus of kinesin heavy chain (Hirokawa et al., 1989). KIF3A has sequence similarity only with the motor domain of kinesin but not with its stalk and tail domain, which are thought to interact with cargoes. This difference suggests that the cargoes of KIF3A may be distinct from those of kinesin.

Taking all the data into consideration, KIF3A and kinesin may bind and transport the same cargoes and be functionally redundant, or alternatively they may bind and transport distinct populations of membranous organelles with the same gravity, thus being beyond the resolution of the sucrose density gradient. In any case, at least two anterograde motor proteins (kinesin and KIF3A) coexist and function in the same axon, indicating that many cargoes are transported anterogradely not by a single motor, but by multiple motors in the axon. The different sensitivities of kinesin and KIF3A to AMP-PNP and further analysis with high resolution electron microscopy with other markers may actually help to identify each cargo transported by its respective motor protein in vivo.

This study showed that although the amount is less, KIF3A is expressed in other tissues as well. Furthermore, sequence analysis of the recently identified novel kinesin-like proteins KLP64D and KLP68D from *Drosophila* revealed them to be homologues and relatives, respectively, of KIF3A (Goldstein, L., personal communication; Pesavento, Stewart, and Goldstein, manuscript in preparation). A kinesin-like protein identified in sea urchin eggs (KRP 85/95) also revealed some similarity with KIF3A (Cole et al., 1993). Therefore, KIF3A may be expressed in many other species in different cell types including neurons. Its function is likely to be important in view of its conservation.

We would like to thank Dr. K. Yoshimura (Zoological Institute, Faculty of Science, University of Tokyo, Tokyo, Japan) for his generous gift of the *Chlamydomonas* and for the technical advice, Dr. N. R. Lomax (National Institutes of Health, Bethesda) for supplying us with taxol, and Mrs. Y. Kawasaki and Ms. H. Sato for their secretarial and technical assistance. The authors thank the monitoring editor and reviewers for their valuable suggestions which improved our manuscript greatly.

This work was supported by a special Grant-in-Aid for Scientific Research from the Ministry of Education, Science and Culture of Japan, and a grant from Rikagaku Kenkyujyo, Wako, Japan to N. Hirokawa.

Received for publication 8 November 1993 and in revised form 14 February 1994.

References

Aizawa, H., Y. Sekine, R. Takemura, Z. Zhang, M. Nangaku, and N. Hirokawa. 1992. Kinesin family in murine central nervous system. *J. Cell Biol.* 119:1287–1296.

Bloom, G. S. 1992. Motor proteins for cytoplasmic microtubules. *Curr. Opin. Cell Biol.* 4:66–73.

Bloom, G. S., M. C. Wagner, K. K. Pfister, and S. T. Brady. 1988. Native structure and physical properties of brain kinesin and identification of the ATP-binding subunit polypeptide. *Biochemistry.* 27:3409–3416.

Bradford, M. M. 1976. A rapid and sensitive method for the quantitation of microgram quantities of protein utilizing the principle of protein-dye binding. *Anal. Biochem.* 72:248–254.

Brady, S. T. 1991. Molecular motors in the nervous system. *Neuron.* 7:521–33.

Brady, S. T., K. K. Pfister, and G. S. Bloom. 1990. A monoclonal antibody against the heavy chain of kinesin inhibits both anterograde and retrograde axonal transport in isolated squid axoplasm. *Proc. Natl. Acad. Sci. USA.* 87:1061–1065.

Cole, D. G., S. W. Chinn, K. P. Wedaman, K. Hall, T. Vuong, and J. M. Scholey. 1993. Novel heterotrimeric kinesin-related protein purified from sea urchin eggs. *Nature (Lond.).* 366:268–270.

Endow, S. A. 1991. The emerging kinesin family of microtubule motor proteins. *Trends. Biochem. Sci.* 16:221–225.

Endow, S. A., and M. Hatsumi. 1991. A multimember kinesin gene family in Drosophila. *Proc. Natl. Acad. Sci. USA.* 88:4424–4427.

Endow, S. A., S. Henikoff, and L. Soler-Niedziela. 1990. A kinesin-related protein mediates meiotic and early mitotic chromosome segregation in Drosophila. *Nature (Lond.).* 345:81–83.

Enos, A. P., and N. R. Morris. 1990. Mutation of a gene that encodes a kinesin-like protein blocks nuclear division in A. nidulans. *Cell.* 60:1019–1027.

Espreafico, E. M., R. E. Cheney, M. Matteoli, A. A. Nascimento, P. V. DeCamilli, R. E. Larson, and M. S. Mooseker. 1992. Primary structure and cellular localization of chicken brain myosin-V (p190), an unconventional myosin with calmodulin light chains. *J. Cell Biol.* 119:1541–1557.

Gho, M., K. McDonald, B. Genetzky, and W. M. Saxton. 1992. Effects of kinesin mutations on neural functions. *Science (Wash. DC).* 258:313–316.

Goldstein, L. S. B. 1991. The kinesin superfamily: tails of functional redundancy. *Trends Cell Biol.* 1:93–98.

Grafstein, B., and D. S. Forman. 1980. Intracellular transport in neurons. *Physiol. Rev.* 60:1167–1283.

Hagan, I., and M. Yanagida. 1990. Novel potential mitotic motor protein encoded by the fission yeast cut7^{+} gene. *Nature (Lond.).* 347:563–566.

Hall, D. H., and E. M. Hedgecock. 1991. Kinesin-related gene unc-104 is required for axonal transport of synaptic vesicles in C. elegans. *Cell.* 65:837–847.

Hirokawa, N. 1982. Cross-linker system between neurofilaments, microtubules, and membranous organelles in frog axons revealed by the quick-freeze, freeze-fracture, deep-etching method. *J. Cell Biol.* 94:129–142.

Hirokawa, N. 1986. 270-K microtubule-associated protein cross-reacting with anti MAP 2 IgG in the crayfish peripheral nerve axon. *J. Cell Biol.* 103:33–39.

Hirokawa, N. 1991. Molecular architecture and dynamics of the neuronal cytoskeleton. In Neuronal Cytoskeleton. R. D. Burgoyne editor. Wiley Liss Inc., New York. 5–74.

Hirokawa, N. 1993. Axonal transport and the cytoskeleton. *Curr. Opin. Neurobiol.* 3:724–731.

Hirokawa, N., and H. Yorifuji. 1986. Cytoskeletal architecture in the reactivated crayfish axons with special reference to the crossbridges between microtubules and membrane organelles and among microtubules. *Cell Motil. Cytoskeleton.* 6:458–468.

Hirokawa, N., G. S. Bloom, and R. B. Vallee. 1985. Cytoskeletal architecture and immunocytochemical localization of microtubule-associated proteins in regions of axons associated with rapid axonal transport: the IDPN-intoxicated axon as a model system. *J. Cell Biol.* 101:227–239.

Hirokawa, N., Y. Shiomura, and S. Okabe. 1988. Tau proteins: the molecular structure and mode of binding on microtubules. *J. Cell Biol.* 107:1449–1459.

Hirokawa, N., K. K. Pfister, H. Yorifuji, M. C. Wagner, S. T. Brady, and G. S. Bloom. 1989. Submolecular domains of bovine brain kinesin identified by electron microscopy and monoclonal antibody decoration. *Cell.* 56: 867–878.

Hirokawa, N., R. Sato-Yoshitake, T. Yoshida, and T. Kawashima. 1990. Brain dynein (MAP 1C) localizes on both anterogradely and retrogradely transported membranous organelles. *J. Cell Biol.* 111:1027–1037.

Hirokawa, N., R. Sato-Yoshitake, N. Kobayashi, K. K. Pfister, G. S. Bloom, and S. T. Brady. 1991. Kinesin associates with anterogradely transported membranous organelles in vivo. *J. Cell Biol.* 114:295–302.

Hollenbeck, P. J. 1989. The distribution, abundance and subcellular localization of kinesin. *J. Cell Biol.* 108:2335–2342.

Hollenbeck, P.J. 1993. Products of endocytosis and autophagy are retrieved from axons by regulated retrograde organelle transport. *J. Cell Biol.* 121:305–315.

Hoyt, H. A., L. He, K. K. Loo, and W. S. Saunders. 1992. Two *Saccharomyces cerevisiae* kinesin-related gene products required for mitotic spindle assembly. *J. Cell Biol.* 118:109–120.

Ingold, A. L., S. A. Cohn, and J. M. Scholey. 1988. Inhibition of kinesin-driven microtubule motility by monoclonal antibodies to kinesin heavy chains. *J. Cell Biol.* 107:2657–2667.

Kitts, P. A., M. D. Ayres, and R. D. Possee. 1990. Linearization of baculovirus DNA enhances the recovery of recombinant virus expression vectors. *Nucleic Acids Res.* 18:5667–5672.

Kohler, G., and C. Milstein. 1976. Derivation of specific antibody-producing tissue culture and tumor lines by cell fusion. *Eur. J. Immunology.* 6:511–519.

Kosik, K. S., L. D. Orecchio, B. J. Schnapp, H. Inoue, and R. L. Neve. 1990. The primary structure and analysis of the squid kinesin heavy chain. *J. Biol. Chem.* 265:3278–3283.

Laemmli, U. K. 1970. Cleavage of structural proteins during the assembly of the head of bacteriophage T4. *Nature (Lond.).* 227:680–685.

Leslie, R. J., R. B. Hird, L. Wilson, J. R. McIntosh, and J. M. Scholey. 1987. Kinesin is associated with a nonmicrotubule component of sea urchin mitotic spindles. *Proc. Natl. Acad. Sci. USA.* 84:2771–2775.

Matsuura, Y., R. D. Posse, and H. A. Overton, and D. H. L. Bishop. 1987. Baculovirus expression vector: the requirements for high level expression of proteins, including glycoproteins. *J. Gen. Virol.* 68:1233–1250.

McDonald, H. B., and L. S. B. Goldstein. 1990. Identification and characterization of gene encoding a kinesin-like gene in Drosophila. *Cell.* 61:991–1000.

Meluh, P. B., and M. D. Rose. 1990. KAR3, a kinesin-related gene required for yeast nuclear fusion. *Cell.* 60:1029–1041.

Navone, F., R. Jahn, G. Di Gioia, H. Stukenbrok, P. Greengard, and P. De Camilli. 1986. Protein p38: an integral membrane protein specific for small vesicles of neurons and neuroendocrine cells. *J. Cell Biol.* 103:2511–2527.

Navone, F., J. Niclas, N. Hom-Booher, L. Sparks, H. D. Bernstein, G. McCaffrey, and R. D. Vale. 1992. Cloning and expression of a human kinesin heavy chain gene: interaction of the COOH-terminal domain with cytoplasmic microtubules in transfected CV-1 cells. *J. Cell Biol.* 117:1263–1275.

Neighbors, B. S., R. C. Williams, Jr., and J. R. McIntosh. 1988. Localization of kinesin in cultured cells. *J. Cell Biol.* 106:1193–1204.

Okabe, S., and N. Hirokawa. 1989. Rapid turnover of microtubule-associated protein MAP 2 in the axon revealed by microinjection of biotinylated MAP 2 into cultured neurons. *Proc. Natl. Acad. Sci. USA.* 86:4127–4131.

Otsuka, A. J., A. Jeyaprakash, J. Garcia-Anoveros, L. Z. Tang, G. Fisk, T. Hartshorne, R. Franco, and T. Born. 1991. The C. elegans unc-104 gene encodes a putative kinesin heavy chain-like protein. *Neuron.* 6:113–122.

Paschal, B. M., and R. B. Vallee. 1987. Retrograde transport by the microtubule associated protein MAP 1C. *Nature (Lond.).* 330:181–183.

Pfister, K. K., M. C. Wagner, D. L. Stenoien, S. T. Brady, and G. S. Bloom. 1989. Monoclonal antibodies to kinesin heavy and light chains stain vesicle-like structures, but not microtubules, in cultured cells. *J. Cell. Biol.* 108:1453–1463.

Ransom, B. R., E. Nende, M. Henkart, P. N. Bullock, and P. G. Nelson. 1977. Mouse spinal cord in cell culture. I. Morphology and intrinsic neuronal electrophysiologic properties. *J. Neurophysiol. (Bathesda)* 40:1132–1150.

Roof, D. M., P. B. Meluh, and M. D. Rose. 1992. Kinesin-related proteins required for assembly of the mitotic spindle. *J. Cell Biol.* 118:95–108.

Sato-Yoshitake, R., Y. Shiomura, H. Miyasaka, and N. Hirokawa. 1989. Microtubule-associated protein 1B: molecular structure, localization, and phosphorylation dependent expression in developing neurons. *Neuron.* 3:229–238.

Sato-Yoshitake, R., H. Yorifugi, M. Inagaki, and N. Hirokawa. 1992. The phosphorylation of kinesin regulates its binding to synaptic vesicles. *J. Biol. Chem.* 267:23930–23936.

Saxton, W. M., M. E. Porter, S. A. Cohn, J. M. Scholey, E. C. Raff, and J. R. McIntosh. 1988. Drosophila kinesin: characterization of microtubule motility and ATPase activity. *Proc. Natl. Acad. Sci. USA.* 85:1109–1113.

Saxton, W. M., J. Hicks, L. S. Goldstein, and E. C. Raff. 1991. Kinesin heavy chain is essential for viability and neuromuscular functions in Drosophila, but mutants show no defects in mitosis. *Cell.* 64:1093–1102.

Schnapp, B. J., T. S. Reese, and R. Bechtold. 1992. Kinesin is bound with high affinity to squid axon organelles that move to the plus-end of microtubules. *J. Cell Biol.* 119:389–399.

Scholey, J. M., M. E. Porter, P. M. Grissom, and J. R. McIntosh. 1985. Identification of kinesin in sea urchin eggs and evidence for its localization in the mitotic spindle. *Nature (Lond.).* 338:355–357.

Scholey, J. M., J. E. Heuser, J. T. Yang, and L. S. B. Goldstein. 1989. Identification of globular mechanochemical heads of kinesin. *Nature (Lond.).* 338:355–357.

Summers, M. D., and G. E. Smith. 1987. A manual of methods for baculovirus vectors and insect cell culture procedures. Texas agricultural experiment station bulletin No. 1555.

Towbin, H., T. Staeherin, and J. Gordon. 1979. Electrophoretic transfer of proteins from polyacrylamide gels to nitrocellulose sheets: procedure and some applications. *Proc. Natl. Acad. Sci. USA.* 85:4350–4354.

Tyler, J. M., and D. Branton. 1980. Rotary shadowing of extended molecules dried from glycerol. *J. Ultrastruct. Res.* 71:95–102.

Ueda, T., P. Greengard, K. Berzins, R. S. Cohen, F. Blomberg, D. J. Grab, and P. Siekevitz. 1979. Subcellular distribution in cerebral cortex of two proteins phosphorylated by a cAMP-dependent protein kinase. *J. Cell Biol.* 83:308–319.

Vale, R. D., B. J. Schnapp, T. S. Reese, and M. S. Sheetz. 1985. Organelle, bead, and microtubule translocations promoted by soluble factors from squid giant axon. *Cell.* 40:559–569.

Witman, G. B. 1986. Isolation of Chlamydomonas flagella and flagellar axonemes. *Methods Enzymol.* 134:280–290.

Yang, J. T., R. A. Laymon, and L. S. B. Goldstein. 1989. A three-domain structure of kinesin heavy chain revealed by DNA sequence and microtubule binding analyses. *Cell.* 56:879–889.

Zhang, P., B. A. Knowles, L. S. B. Goldstein, and R. S. Hawley. 1990. A kinesin-like protein required for distributive chromosome segregation in Drosophila. *Cell.* 62:1053–1062.